Investigating the Fermi motion effects on the incoherent DVCS channel

February 20, 2017

In our DVCS analysis, we considered the initial proton of the incoherent channel to be at rest, while this is not totally true because of the Fermi motion. Does this assumption is a good approximation? what other options can be used to minimize this effect on the calculated exclusive quantities?

Figure 1 presents the leading order handbag diagram of the incoherent DVCS channel off ^{4}He, where the nucleus breaks and the DVCS occurs on a bound nucleon. Ideally, the transferred momentum squared (t) is defined using the initial and the final nucleons' 4-vectors as $(p - p')^2$. Then as a DVCS requirement, t has to be greater than a certain value (t_{min}), that is defined using the kinematics of the incoming and the scattered electrons. Due to the knowledge lack of the initial proton's momentum, this cut maybe inaccurate causes loosing some good DVCS events. In this work, we try to tackle this issue and check the stability of the reconstructed beam-spin asymmetry, as being our DVCS observable.

Typically, the transferred momentum squared t is equal to the transferred momentum squared (t') defined between the virtual photon and the final-state real photon, as shown in Figure 1. While defining the momentum transferred as t' is a good way to pass the Fermi motion effect on the initial bound proton, it is more smeared than than t due to bigger energy resolutions of the photons. Figure 2 shows the distributions of the coherent and the incoherent relative difference between t and t'. One can see that the coherent DVCS channel, the distributions is symmetric and centered at zero as expected due to our good knowledge on the initial ^{4}He target, while it is not exactly the case for the incoherent case due to the Fermi motion.

In the following, we check the effects of defining the transferred momentum squared as t and t' on the exclusive distributions and on the reconstructed beam-spin asymmetries. Figure 3 presents the exclusive distributions of the incoherent DVCS events where the transferred momentum squared is defined as t, while it is define as t' in figure 4. To minimize the smearing effects of t' on the exclusive distributions, 2σ exclusive cuts were optimized compared to 3σ cuts which were applied in the t case. In terms of collected statistics, the 2σ cuts using t' gave almost the same statistics using t. From comparing the exclusive distributions, especially the $ep\gamma$ missing energy and the missing mass squared, one sees that using t' gives more Gaussian missing energy distributions and cleaner missing mass squared distribution.

Figure 5 shows our measured incoherent beam-spin asymmetries, for the three sets of the two-dimensional bins, in the two scinarios of defining the transferred momentum squared. The Q^2, x_B, and $-t$-dependencies of A_{LU} at ϕ= 90° (the α parameter of the fit) are shown in figure 6.

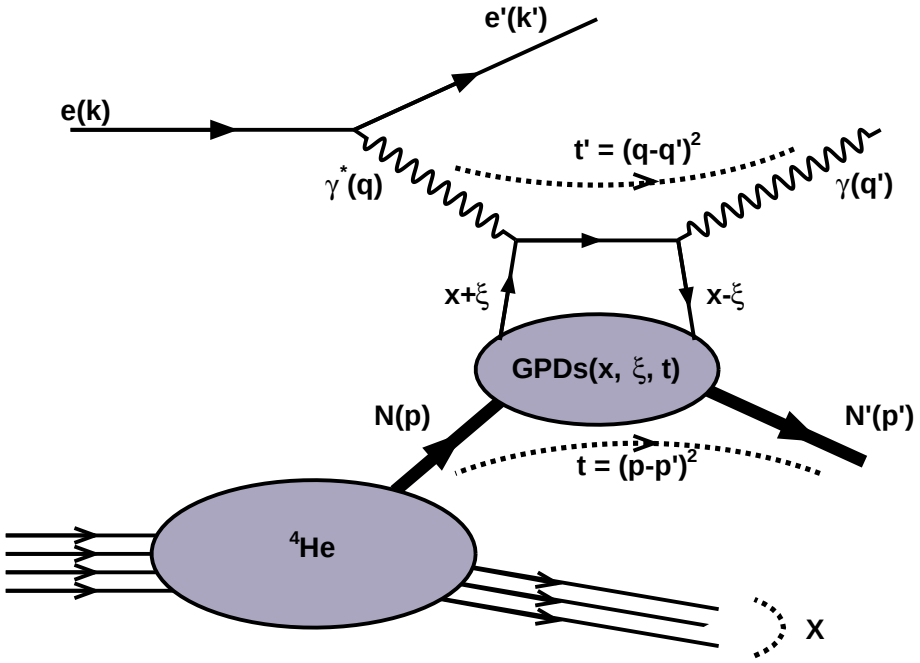

Figure 1: Representation of the leading order handbag diagram of the incoherent DVCS process off ^{4}He

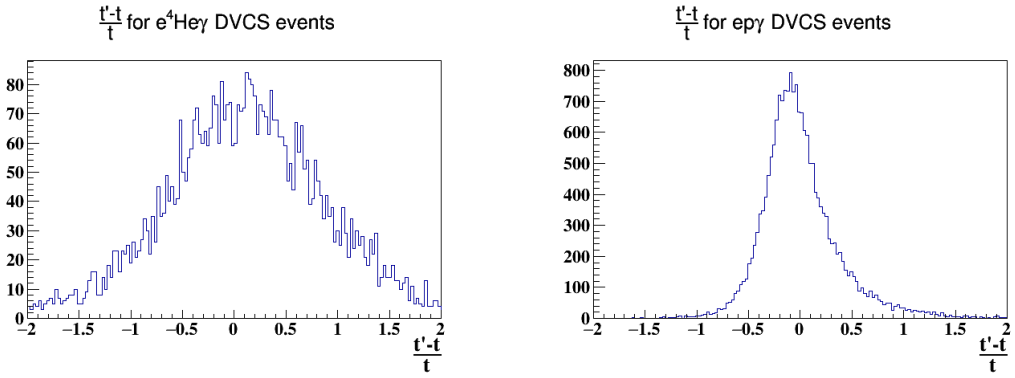

Figure 2: On the left: the coherent relative difference between t and t'. On the right: the incoherent relative difference.

Conclusions

In summary, we have studied the effects of Fermi motion on the measured incoherent beam-spin asymmetries by defining the transferred momentum squared through the nucleons in one case and through the photons in the other case. In terms of collected statistics, 2σ exclusive cuts using the photons produced the same statistics as 3σ cuts. The exclusive distributions using t', through the photons, have shown more acceptable distributions in terms of being more symmetric in some cases and cleaner on others. The reconstructed asymmetries in the two cases of defining the transferred momentum squared are compatible and while the given error bars. As a suggestion, we would like to consider the t' analysis as the final set for publications unless a major objections appear.

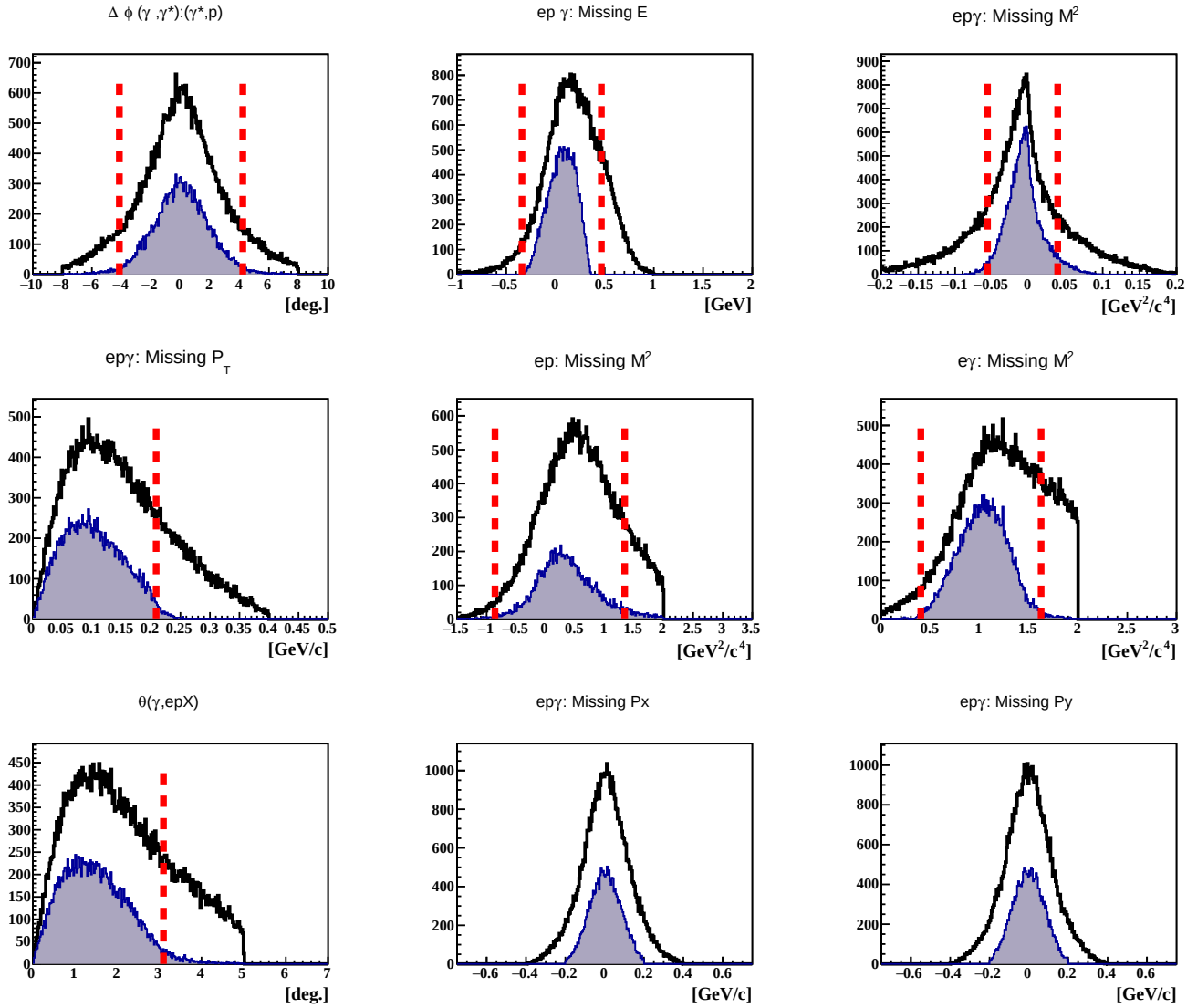

Figure 3: The old set of exclusive cuts with t>t_{min}. The black distributions represent the incoherent DVCS events candidate. The shaded distributions represent the events which passed all the exclusivity cuts except the quantity plotted. The vertical red lines represent the applied exclusivity, 3σ cuts.

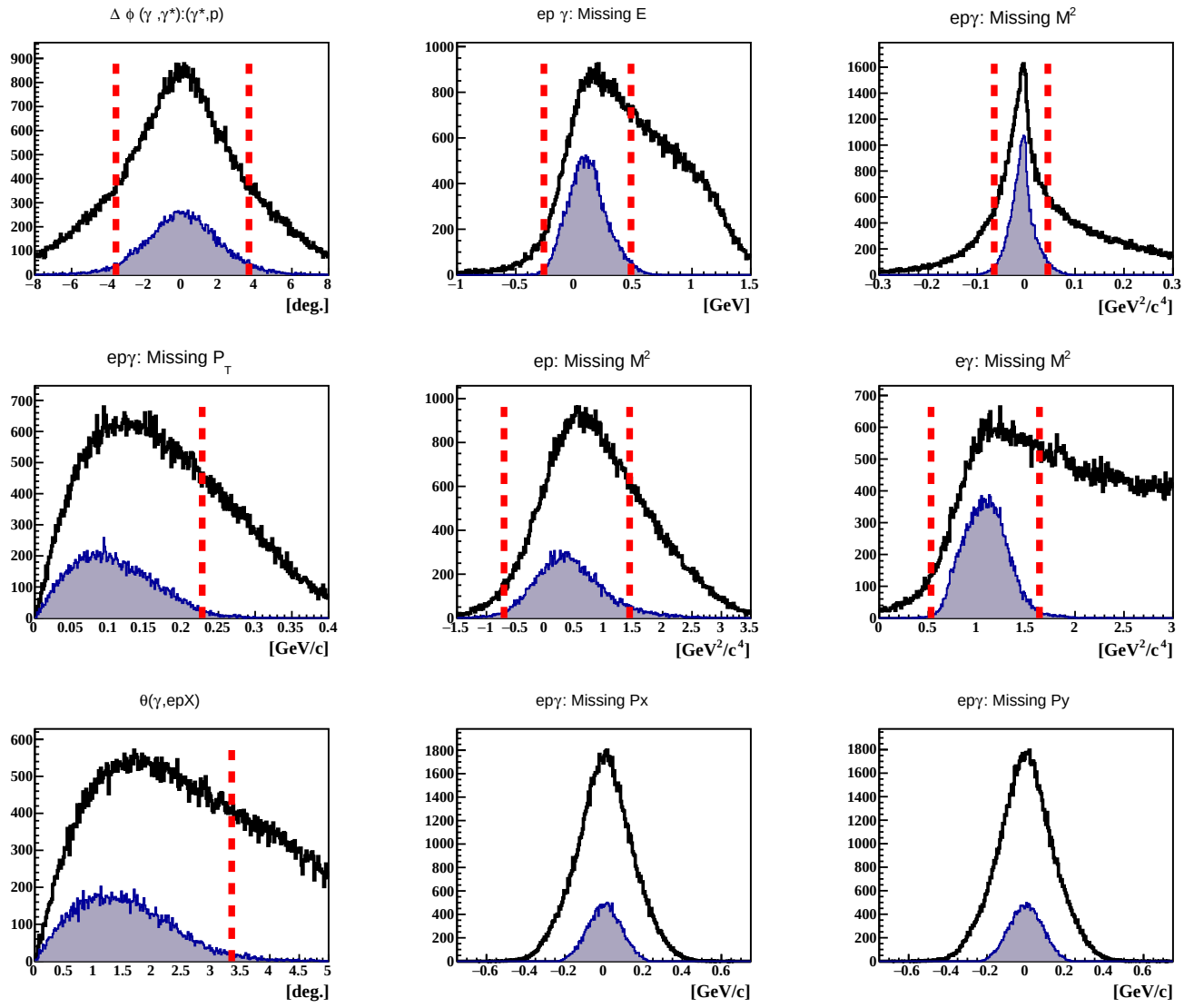

Figure 4: New set of exclusive cuts with t'>t_{min}. The black distributions represent the incoherent DVCS events candidate. The shaded distributions represent the events which passed all the exclusivity cuts except the quantity plotted. The vertical red lines represent the applied exclusivity, 2σ cuts.

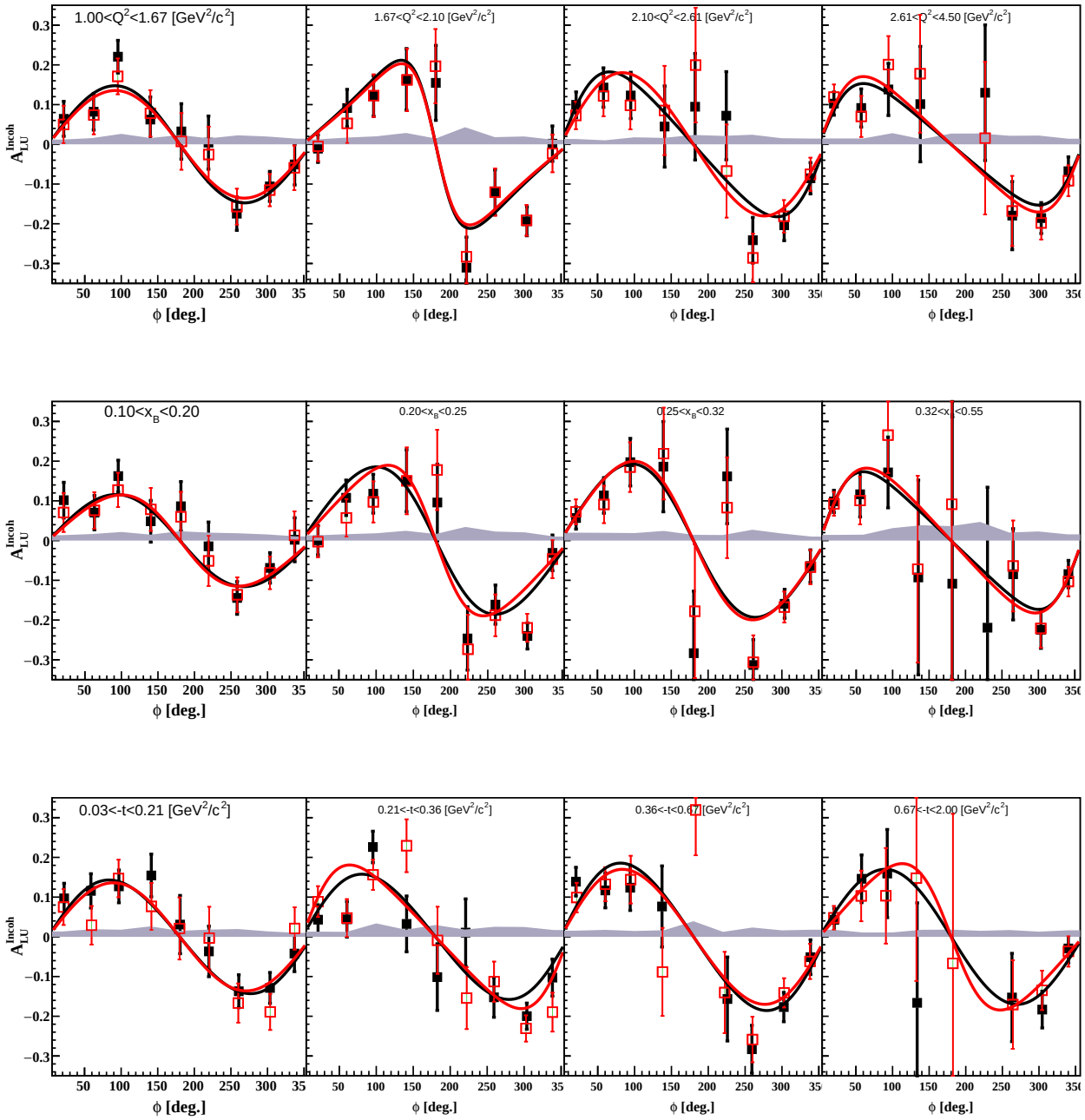

Figure 5: The reconstructed incoherent A_{LU} as a function of the angle ϕ in Q^2, x_B, and $-t$ bins, respectively from top to bottom using t>t_{min} in black squares, and t'>t_{min} in red squares.

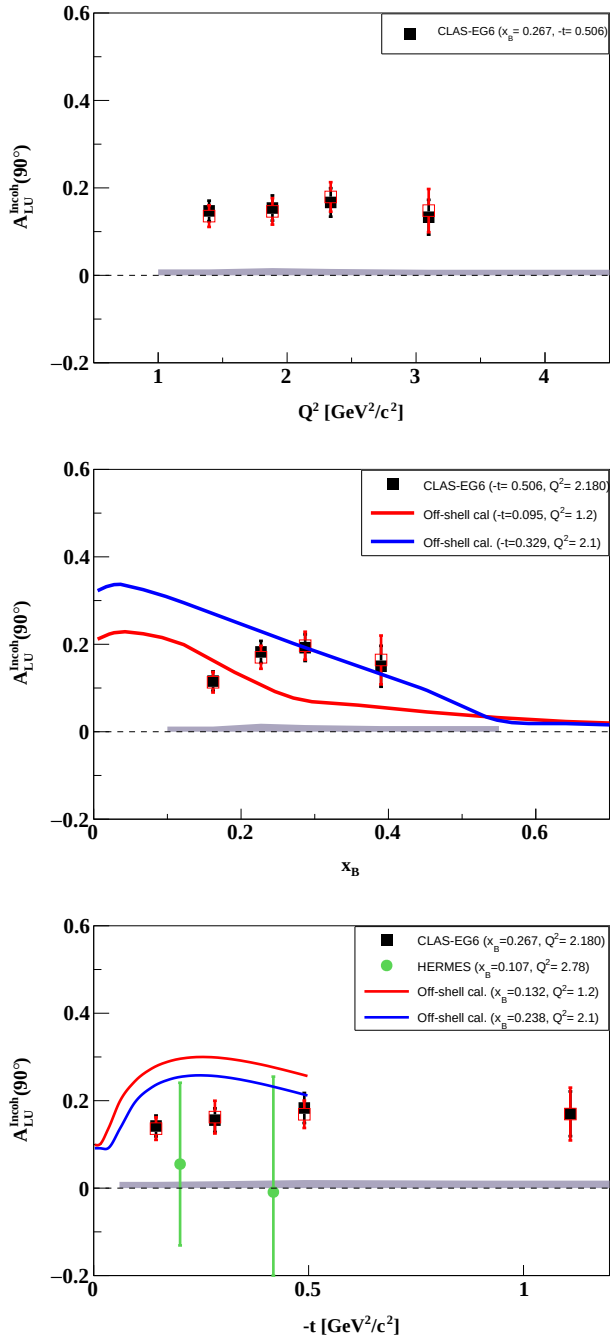

Figure 6: The Q^2 (top), x_B (middle), and $-t$-dependencies (bottom) of the incoherent A_{LU} at $\phi = 90^\circ$, using the t>t_{min} cut and the corresponding exclusive cuts in black squares, and in red squares using the t'>t_{min} and it's exclusive cuts. The curves are theoretical calculations. On the bottom: the green circles are the HERMES $-A_{LU}$ (positron beam was used) inclusive measurements.